Physical and Chemical Properties of Polypyrrole–Carbon Fiber Interphases Formed by Aqueous Electrosynthesis

JUDE O. IROH* and GREG A. WOOD

Materials Science and Engineering Department, College of Engineering, University of Cincinnati, 498 Rhodes Hall (ML 12), Cincinnati, Ohio 45221-0012

SYNOPSIS

The properties of carbon fibers modified by aqueous electrochemical synthesis of pyrrole has been determined by using the dynamic contact angle analyzer (DCA), scanning electron microscopy (SEM), and Fourier transform infrared spectroscopy (FTIR). Electrochemical process parameters such as the initial pyrrole concentration, electrolyte concentration, applied voltage, electrolyte type, and reaction time were systematically varied, and their impact on the polypyrrole–carbon fiber interphases surface free energy and morphology was ascertained. The surface free energies of the polypyrrole–carbon fiber interphases were obtained by using single fiber filaments. SEM analysis of the interphases revealed several distinct surface structures, including smooth, porous, granular, microspheroidal, and leafoidal morphologies. The noncoated but commercially surface oxidized carbon fibers have smooth surface morphology with occasional longitudinal striations. FTIR analysis of the polypyrrole interphases confirmed that the counterions derived from the electrolytes were incorporated into the film. The surface free energies of the electrochemically formed polypyrrole–carbon fiber interphases equivalent to 60–75 dynes/cm, was determined to be up to 40% higher than that for the surface oxidized but unsized carbon fibers equivalent to 50 dynes/cm. This improvement in the surface free energies of the polypyrrole–carbon fiber interphases suggests easy wettability by polymer matrices such as epoxy resin, $\gamma \sim 47$ dynes/cm and, polyimide matrix, $\gamma \sim 45$ dynes/cm.

INTRODUCTION

The modification of carbon fibers by the application of electropolymerized coatings has been shown to result in significant improvement in the mechanical properties of the electrocoated fiber-epoxy resin composites.[1-4] The adhesion between the fibers and a polymer matrix determines the interfacial and mechanical properties of advanced composites.[5,6] The adhesion between the two phases may be ascribed to chemical interaction (including covalent bonding) and physical effects such as mechanical interlocking and interdiffusion between the phases.[7,8] The surface free energy of fibers is an important indicator of their wettability by a matrix resin. Adequate wetting of the fibers by the matrix is a necessary condition for adhesion between the two components. Surface energy can be defined as the change in free energy when the surface area of a medium is increased by unit area.[9] The relationship between the surface free energy of a solid, the surface energy of a liquid, and the interfacial energy is given by Young's equation:[10]

$$\gamma_{LV} \cdot \cos\theta = \gamma_{SV} - \gamma_{SL} \quad (1)$$

where γ_{LV} is the surface energy of a liquid in equilibrium with the saturated vapor of the liquid, θ is the contact angle, γ_{SV} is the surface free energy of a solid in equilibrium with the saturated vapor of the liquid, and γ_{SL} is the interfacial energy between the solid and liquid.

Generally, the lower the contact angle of a liquid on a solid, the better the wettability of the solid. One of the goals of fiber modification processes is to increase the surface energy of the fibers and

* To whom correspondence should be addressed.

Journal of Applied Polymer Science, Vol. 62, 1761–1769 (1996)
 CCC 0021-8995/96/101761-09

thereby improve their wettability by and adhesion with the matrix.

One of the techniques used to determine the surface free energy of fibers is the modified Wilhelmy technique. A dynamic contact angle analyzer, DCA-322 equipped with a micro balance, is used to determine the contact angle and surface free energy of the fibers using water and glycerol as solvents. A combination of a low contact angle ($\theta \leq 30$ degrees) and high surface free energy ($\gamma \geq 45$ dynes/cm) will imply adequate wetting of the substrate. Experimentally, a beaker containing a solvent of known surface energy, (water/glycerol) will be mounted on the micro balance. The fiber(s) to be analyzed is attached to a titanium alloy bar, and the setup is then be lowered into the solvent until a predetermined depth ($\sim$ 10 mm) is reached. The substrate is then withdrawn, and the cycle repeated. The force F required to push/pull the substrate (thickness/diameter d) into/from the solvent of known surface energy γ_{LV} is monitored by the micro balance and used to calculate the advancing/receding contact angle θ:

$$F = (\pi d \cdot \gamma_{LV} \cdot \cos\theta) \tag{2}$$

The work of adhesion, W_A can be related to the liquid surface energy and the contact angle by the following expression:

$$W_A = (1 + \cos\theta)\gamma_{LV} \tag{3}$$

Both the geometric mean equation (eq. 4) and the Harmonic mean equation (eq. 5) are used to relate the dispersive and polar surface energies, γ^d and γ^p, respectively, to the work of adhesion:

$$W_A = 2[(\gamma_c^d\gamma_s^d)^{1/2} + (\gamma_c^p\gamma_s^p)^{1/2}] \tag{4}$$

$$W_A = 4\left[\frac{\gamma_c^d\gamma_s^d}{\gamma_c^d + \gamma_s^d} + \frac{\gamma_c^p\gamma_s^p}{\gamma_c^p + \gamma_s^p}\right] \tag{5}$$

where the subscripts c and s represent the coating and the substrate, respectively.

For a poorly polar coating, the work of adhesion, $W_A = W^d + W^p$ can be related to the interfacial shear strength τ by combining the Schultz and Nardin and modified Cox expressions[11–13]:

$$\tau = kW_A = k(W^d + W^p) = \left(\frac{E_c}{E_s}\right)^{1/2}\frac{W_A}{\lambda} \tag{6}$$

where λ is the equilibrium intermolecular center-to-center distance and has a value of $\sim$ 0.5 nm.[14] E_c and E_s are the elastic modulii of the coating and the substrate, respectively.

The work of adhesion $W_A = \gamma_s + \gamma_c - \gamma_{sc}$ can be compared with the work of cohesion of the coating, $W_c = 2\gamma_c$. The interfacial surface free energy γ_{sc} can be calculated from the following relationship:

$$\gamma_{sc} = \gamma_s + \gamma_c - 2\sqrt{\gamma_s^d\gamma_c^d} \tag{7}$$

If the work of adhesion is larger than the work of cohesion, then interfacial failure will not occur. The work of adhesion and the work of cohesion will be measured before and after exposure of the samples to oxidative–corrosive conditions to assess the impact on the film and film–substrate interaction. This approach will provide an indirect assessment of the effect of corrosion on the adhesion between the polymeric coating and the substrate.

An extended version of eq. (2) includes a buoyancy correction term. To eliminate the buoyancy correction, a plot of the immersion force F against the immersion depth d is constructed. The immersion depth is extrapolated to zero depth, $d = 0$ (where the sample just touches the surface of the liquid), thus eliminating the need for this correction (eq. 2). This is automatically done by the Wilhelmy plate/balance. A probe liquid of very low surface tension such as hexadecane ($\gamma \sim 27.6$ dynes/cm) is used to determine the perimeter of the substrate. It is believed that a liquid with a low surface tension will spread spontaneously on a solid with high surface tension ($\theta \sim 0$ and $\cos\theta \sim 1$).

Drzal used energetic ion radiation of polyethylene fibers to improve the adhesion between the fibers and an epoxy resin.[15] He noted that wetting of the fibers was improved when the surface energy of the fibers was increased with respect to the matrix. They determined the contact angles of polar and nonpolar liquids on polyethylene single fibers by the tensiometric technique.[15] A similar procedure is described elsewhere.[16] Kaelble and Dynes also used the micro-Wilhelmy plate method to study the effect of surface treatments on graphite fibers.[17] Tissington et al. determined the contact angles of epoxy resin placed on single fiber filaments, by visual inspection of the shapes of drops of the resin on the fibers.[18] Finally, Wagner reported a numerical approach for the determination of the contact angles.[19]

Other researchers have determined the wettability of surface modified carbon fibers. Chiu et al. used the resin drop method to determine the contact angles of epoxy resin on polypyrrole coated carbon fibers.[20] They found that the application of polypyrrole coatings onto the fibers decreased the contact

Table I Electropolymerization Process Parameters

Sample	Concentration of Pyrrole (mol/L)	Electrolyte[a]	Concentration of Electrolyte (mol/L)	Applied Voltage (*V*)	Time (min)
1-2c	0.1	T_4SNa	0.25	1.5	5
1-5c	1.5	T_4SNa	0.25	1.5	5
2-2c	0.5	T_4SNa	0.10	1.5	5
2-5a	0.5	T_4SNa	1.50	1.5	.5
2-5c	0.5	T_4SNa	1.50	1.5	5
3-2c	0.5	T_4SNa	0.25	0.5	5
3-5c	0.5	T_4SNa	0.25	2.5	5
6-2c	0.5	DbSNa	0.01	1.5	5
6-4a	0.5	DbSNa	0.25	1.5	.5
6-4c	0.5	DbSNa	0.25	1.5	5
7-2c	0.5	DbSNa	0.10	0.5	5
7-5c	0.5	DbSNa	0.10	2.5	5
8-2c	0.1	DbSNa	0.10	1.5	5
8-4c	1.5	DbSNa	0.10	1.5	5
9-2c	0.1	H_2SO_4	0.25	1.5	5
9-5c	1.5	H_2SO_4	0.25	1.5	5
10-2a	0.5	H_2SO_4	0.05	1.5	.5
10-2c	0.5	H_2SO_4	0.05	1.5	5
10-4c	0.5	H_2SO_4	0.50	1.5	5
11-2b	0.5	H_2SO_4	0.10	0.5	5
11-5b	0.5	H_2SO_4	0.10	2.5	5

[a] T_4SNa, toluene-4-sulfonic acid sodium salt; DbSNa, dodecylbenzene-sulfonic acid sodium salt; H_2SO_4, sulfuric acid.

angle of epoxy resin on the fibers and hence improved their wettability. They did not determine the surface energy of the coated fibers.

In this paper, we report the surface energy and the morphology of carbon fibers coated with polypyrrole by aqueous electrochemical polymerization. The goal is to improve the wettability of polypyrrole modified fibers by polymers such as epoxy resin and polyimide. Many process parameters, such as the pyrrole concentration, the electrolyte concentration, the type of electrolyte, the applied voltage, and the electropolymerization time were systematically varied, and their effect on the surface energy of the coated fibers was determined.

The dynamic contact angle analyzer (DCA) was used to determine the surface energies of the carbon fibers. The DCA is sensitive enough to measure the perimeter of and the force required to advance or recede a single fiber to and from a certain depth in a liquid of known surface tension. The use of this technique eliminates the problems often encountered with other methods in which liquids form inconsistent shapes on some thin fibers or at least make measurement difficult due to both the small radius of curvatures and the meniscus.[10]

EXPERIMENTAL

The carbon fibers used in this study were T650/35 Thornel PAN based fibers donated by Amoco Performance Products Inc. The instrument used to coat the fibers was an EG&G Princeton Applied Research Potentiostat/Galvanostat Model 273A. The coating was carried out in a three compartment polypropylene cell. The carbon fibers were used as the working electrode. They were placed in the center compartment of the cell. The two outer counter electrode compartments of the cell each contained a titanium alloy plate counter electrode. The pyrrole and electrolyte concentration were varied from 0.01 to 1.5*M*. Applied voltage of the range of 0.1 to 2.5 V was used. Electropolymerization was performed for 30 to 1200 s. Three different electrolytes were used in this work, namely toluene-4-sulfonic acid sodium salt (T_4SNa), dodecylbenzene–sulfonic acid sodium salt (DbSNa), and sulfuric acid (H_2SO_4). Table I shows the process parameters used in the determination of the surface energy of single fibers. The surface energy of the fibers was determined by using a CAHN Dynamic Contact Angle Analyzer, Model 322. The coatings formed by using a high and

Table II Surface Free Energies of the Commercial Nonsized but Surface Oxidized T-650 Carbon Fibers and the Polypyrrole-T-650 Carbon Fiber Interphases Formed in Different Electrolytes

Sample ID	Electrolyte Type	Surface Free Energy (dynes/cm)
1-2c	T_4SNa	65.92
1-5c	T_4SNa	70.95
2-2c	T_4SNa	69.84
2-5a	T_4SNa	73.09
2-5c	T_4SNa	63.17
3-2c	T_4SNa	71.68
3-5c	T_4SNa	68.84
6-2c	DbSNa	58.01
6-4a	DbSNa	63.62
6-4c	DbSNa	62.67
7-2c	DbSNa	53.61
7-5c	DbSNa	51.88
8-2c	DbSNa	63.35
8-4c	DbSNa	60.33
9-2c	H_2SO_4	50.85
9-5c	H_2SO_4	59.21
10-2a	H_2SO_4	59.78
10-2c	H_2SO_4	52.27
10-4c	H_2SO_4	63.48
11-2b	H_2SO_4	66.60
11-5b	H_2SO_4	64.80
Noncoated carbon fiber	Nil	51.0

low process parameter, respectively, were selected for analysis. The surface energy of the test liquids were determined by the Wilhelmy plate method, and the surface free energies of the as received carbon fibers and the polypyrrole–carbon fiber interphases were calculated by the geometric mean method.

Individual single filament fibers of approximately 4 cm in length were extracted from a coated fiber bundle. The fiber was attached to the DCA by means of a titanium alloy wire holder using a masking tape. The perimeter and diameter of the single fibers were determined in hexadecane, which completely wets the fibers. The fiber was positioned about 5 mm above the surface of the probe liquid and lowered at a rate of 20 μm/s into the liquid. At an immersion depth of about 5 mm, the motion was reversed, and the fiber was withdrawn from the probe liquid. The total run time was near 17 min. The device measured the force as a function of position and calculates the contact angles from the advancing and receding curves. The surface free energy of the single fiber filament is determined by using the surface energy of the probe liquids and the cosine of the contact angle. Three single fiber filaments were tested for each fiber bundle, and the results were averaged.

RESULTS AND DISCUSSION

The higher the surface energy of a solid, the higher is the solid's wettability by a liquid. The spreading of a liquid on a solid occurs spontaneously when the contact angle of the liquid on the solid approaches zero (eq. 1). Adequate wetting of reinforcements by the matrix is a necessary condition for good fiber-matrix adhesion.

The polypyrrole-coated carbon fibers have higher surface free energies than the noncoated (surface oxidized) carbon fibers (Table II). The surface free energy of the noncoated carbon fibers was determined to be $\sim$ 51 dynes/cm. The reproduceability of the data is shown in Figure 1. The surface free energies obtained from three different DCA measurements using noncoated single fiber filaments were of the same magnitude (Fig. 1). Surface energy values of 41–56 dynes/cm were reported for various treated carbon and graphite fibers.[16,17] Note that all the fibers electrocoated with polypyrrole have surface energies significantly higher than that of the noncoated fibers (Table II). It is believed that the polypyrrole–carbon fiber interphases will be easily wetted by resins such as Epon 828 epoxy resin (γ

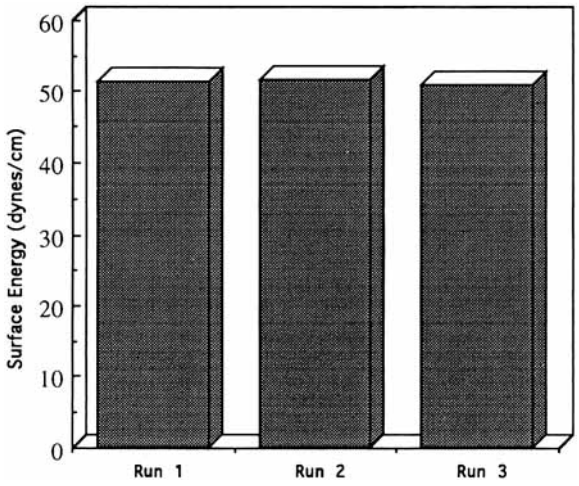

Figure 1 Reproducibility of the surface free energy measurement of noncoated single filament T-650 carbon fiber.

= 47.5 dynes/cm),[15] nylon 6,6 ($\gamma \sim 45$ dynes/cm), and polyimide resin ($\gamma \sim 40$–50 dynes/cm)[21] by virtue of their higher surface energies ($50 < \gamma \geq 70$ dynes/cm). The improved wettability of the electrocoated fibers should translate into an improvement in the mechanical and interfacial properties of the coated fiber–epoxy/polyimide composites.

The effect of the applied voltage and the electropolymerization time on the surface free energy of the coated fibers is shown in Figures 2 and 3, respectively. Three pairs of data, along with a bar for the uncoated fibers for comparison, are presented. Each data pair corresponds to samples coated using the same supporting electrolyte. No significant change in the surface free energy of the polypyrrole–carbon fiber interphases occurred as a result of the 80% increase in the applied voltage. Figure 3 shows the relationship between the electropolymerization time and the surface free energy of the interphases. The polypyrrole interphases formed in a duration of 30 s had slightly higher surface free energy than those formed in 300 s. The surface free energy of the interphases formed in T_4SNa and H_2SO_4, respectively (surface morphology ranged from microspheroidal to leafoidal and smooth), decreased by about 16% as the reaction was increased by 80%; however, those formed in DbSNa (predominantly smooth morphology) showed no change in the surface free energy as a function of reaction time. The slight variation in surface free energy of the polypyrrole interphases may be attributed to the surface morphology of the coatings.

The chemical composition of the polypyrrole–carbon fiber interphases was determined by FTIR.

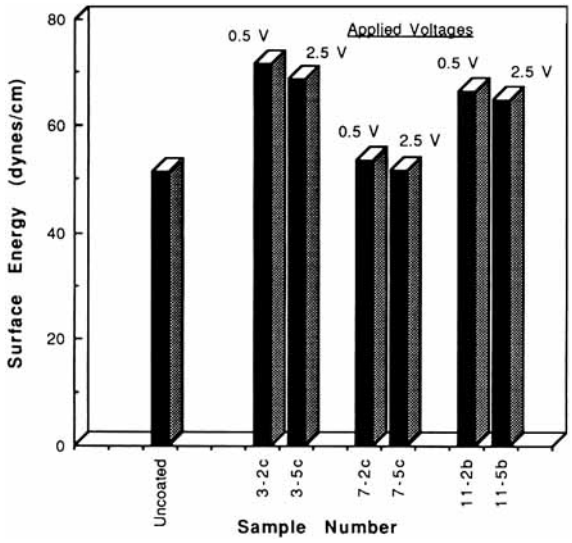

Figure 2 Surface free energies of polypyrrole–carbon fiber interphases formed by using low and high applied voltages as a function of the electrolyte. Samples 3-2c and 3-5c for T_4SNa, 7-2c and 7-5c for DbSNA, and 11-2b and 11-5b for H_2SO_4 as the supporting electrolytes.

The IR spectra of the polypyrrole interphases extracted from the carbon fibers show the characteristic IR peaks associated with pyrrole and the counterions derived from the electrolytes used in electrosynthesis. Figure 4 shows the comparison of IR spectra for pyrrole (Fig. 4, bottom) and that for

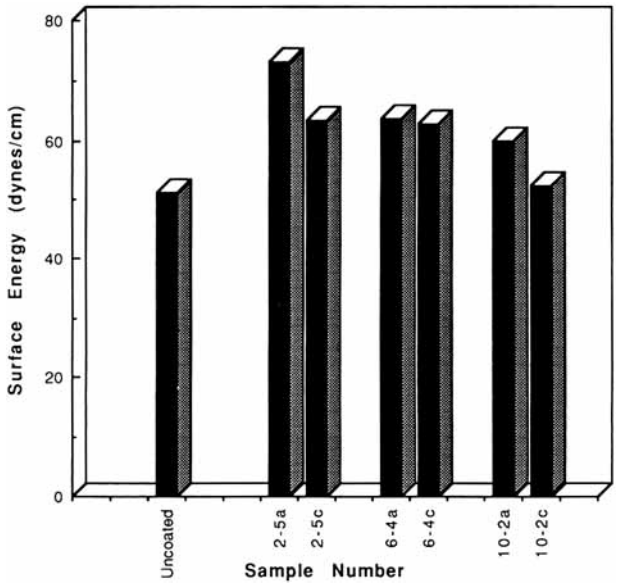

Figure 3 The effect of short electropolymerization time on the surface free energy of polypyrrole–carbon fiber interphases (left bar of each pair, 30 s; right bar, 5 min). Electrolytes used: 2-5a and 2-5c for T_4SNa; 6-4a and 6-4c for DbSNa; 10-2a and 10-2c for H_2SO_4.

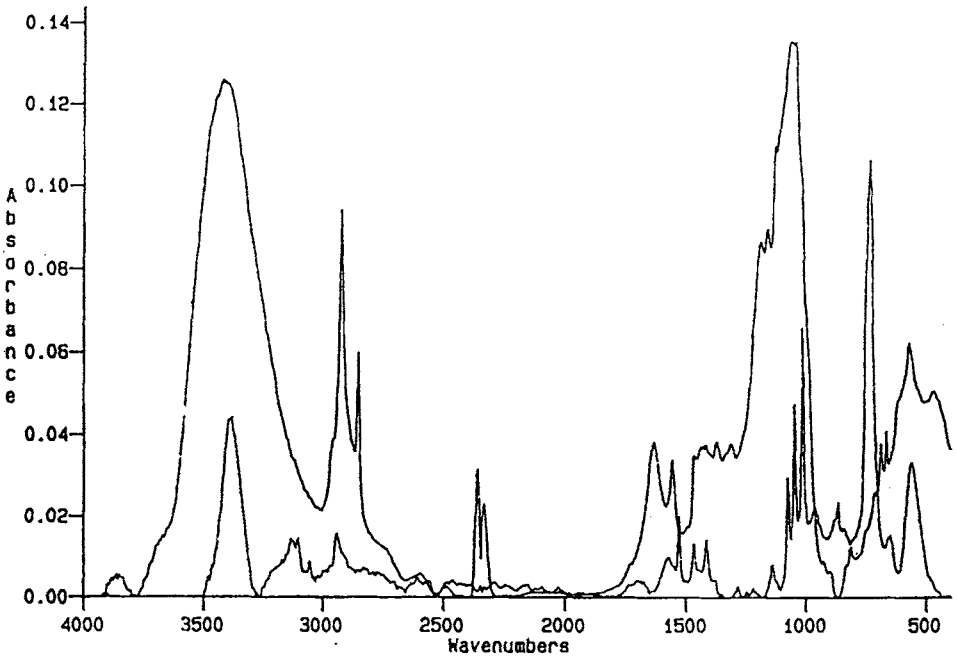

Figure 4 Infrared spectra of pyrrole monomer (lower) and a typical polypyrrole interphase, 1-2e (upper), formed by using DbSNa as the electrolyte.

the polypyrrole interphase formed in DbSNa solution (1-2e) (Fig. 4, top). The broad peak occurring at 3200–3500 cm^{-1} corresponds to the N—H stretching in the pyrrole ring.[22,23] The IR peaks appearing in the 3100's cm^{-1} are due to the aromatic C—H stretches.[22,24] The strong absorption peak at 2940 cm^{-1} is due to the vibration of either an R—CH_2—R group or a R—CH_2 group.[24] The IR peaks occurring between 1700 and 1100 cm^{-1} correspond to C—C stretches, C—H deformations, C—N stretches, N—H deformation, and C=C stretches.[16] Three distinct bands appear near 1100–1000 cm^{-1} and are reported to be due to C—H deformations.[22] The remaining region, 1000–400 cm^{-1}, is dominated by a strong peak near 735 cm^{-1}, which is due to a C—H wag vibrations coming from adjacent hydrogen atoms on a ring compound.[22,24] There is also a peak near 565 cm^{-1} that probably corresponds to an N—H wag vibration. The remaining peaks in this region can be assigned vibrations such as other C—H wags and a couple of different ring vibrations. The IR spectra of the polypyrrole interphases (Fig. 4, top) confirmed the presence of the electrolyte in the coatings. One of the striking features of the 1-2e spectrum (Fig. 4, top) is the large peak region located between 1100–1000 cm^{-1}. The sulfonic acid salts show four characteristic peaks near 1230, 1190, 1130, and 1040 cm^{-1}, which correspond to three SO groups and one S-phenyl vibration.[25] Overall, the IR analysis shows that the counterion derived from the electrolyte is embedded in the coatings.

The surface morphology of the electrochemically formed polypyrrole–carbon fiber interphases varied with the electrolyte used. As a result, an attempt was made to correlate the surface free energy of the interphases to the surface morphology. The morphology of the polypyrrole interphases was classified as smooth, microspheroidal, leafoidal, and porous/granular [Fig. 5(a–d)]. The correlation of the surface free energies with the polypyrrole interphase morphologies are shown in Figure 5. The polypyrrole interphases having microspheroidal morphology had higher surface free energy than the polypyrrole interphases with smooth morphology. The coatings with microspheroidal morphology were formed by using T_4SNa and H_2SO_4, respectively, as the electrolyte. The polypyrrole–carbon fiber interphases with smooth morphology have slightly lower surface energies. Diaz et al. reported that physical structure differences of the surfaces of thin films formed by either plasma or electrochemical polymerization did not affect the surface energies of the films.[26] Figure 6 shows the surface free energy of polypyrrole–carbon fiber interphases as a function of the electrolyte type and other process parameters. The initial concentration of the electrolytes in the reaction cell did not have any significant influence on the surface

A) Uncoated single carbon fiber

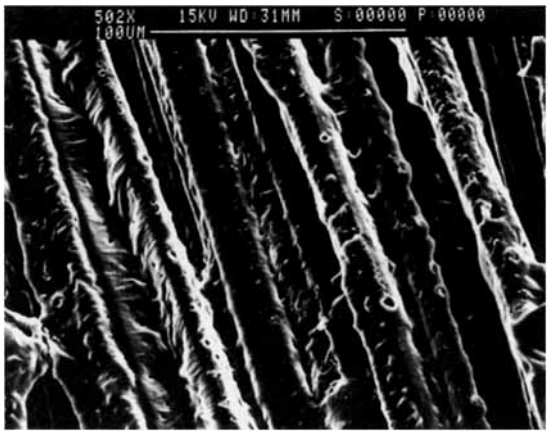

C)

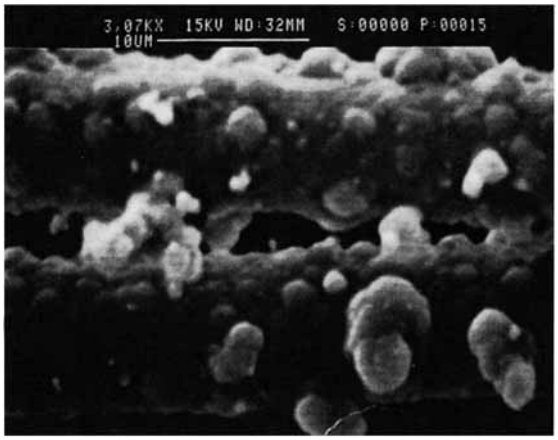

B)

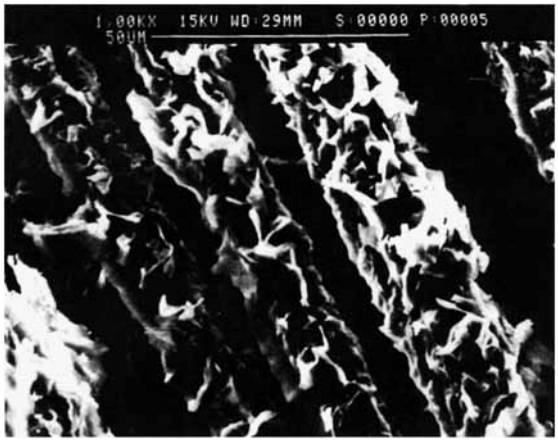

D)

Figure 5 SEM micrographs of the morphologies of (A) surface-oxidized but noncoated carbon fibers and (B, C, D) polypyrrole–carbon fiber interphases.

free energy of the interphases. The polypyrrole interphases formed in T_4SNa solution, however, showed higher overall surface free energies.

Figure 7 shows the surface free energies of the polypyrrole interphases as a function of the electrolyte and electrolyte concentration. The coatings containing toluene sulfonate counterions (mostly microspheroidal morphology) have higher surface free energies than those that contain dodecylbenzene sulfonate counterions (mostly smooth morphology) or H_2SO_4 (mixed morphologies). Examination of Figure 7 and Tables I and II shows that the sample pairs 1-2c and 9-2c, as well as 1-5c and 9-5c, were formed by using the same process parameters. T_4SNa and H_2SO_4, however, were used to form 1-2c–1-5c and 9-2c–9-5c interphases, respectively. The polypyrrole interphases formed in a T_4SNa solution have higher surface free energies. Comparison between T_4SNa and DbSNa reveals that both electrolytes contain similar chemical structure. However, the dodecyl substituent $-(CH_2)_{11}-CH_3$ contained in DbSNa is much longer than the methyl $-CH_3$ substituent on T_4SNa. This basic difference in the structure of these electrolytes may be responsible for the differences in the morphology and surface free energies of the derived interphases. The IR result is confirmed by elemental analysis of representative coating samples. A mole ratio of 3 : 1 for pyrrole : T_4SNa and pyrrole : DbSNa and near 5 : 1 for pyrrole : H_2SO_4 was determined by elemental analysis (Fig. 8).[27]

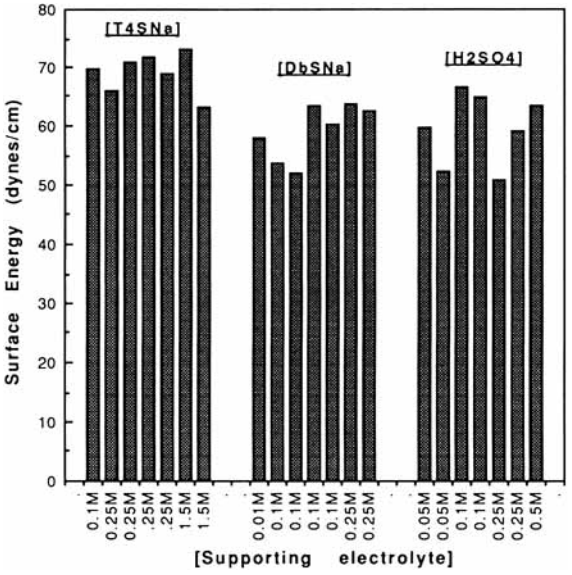

Figure 6 Surface free energies of the polypyrrole–carbon fiber interphases as a function of the initial electrolyte concentration.

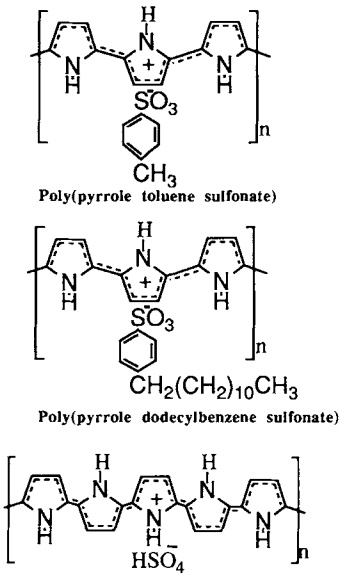

Figure 8 Representation of doped polypyrrole formed on carbon fibers.

CONCLUSION

The properties of polypyrrole–carbon fiber interphases formed by electrochemical synthesis have been investigated. Polypyrrole was formed onto carbon fibers by electrosynthesis, and the composition, morphology and surface free energy of the resulting coatings were determined. The surface free energy of the polypyrrole interphases was correlated with the electrochemical process parameters such as the pyrrole concentration, applied voltage, electrolyte concentration, electrolyte type, and reaction time. Overall, the electrosynthesized polypyrrole–carbon fiber interphases had higher surface free energies 50 $< \gamma \geq 65$ dynes/cm than the commercially surface oxidized but nonsized carbon fibers. IR analysis of the polypyrrole interphases showed that part of the electrolytes (counterions) was incorporated into the interphase. Polypyrrole-coated carbon fibers with microspheroidal morphology showed highest surface energy. The polypyrrole interphases formed in T_4SNa solution had higher surface free energies than those formed in either DbSNa or H_2SO_4 solution. The electrolyte concentration did not seem to have any significant impact on the surface free energy of the coated fibers. The differences in the morphology and surface free energies of polypyrrole–carbon fiber interphases formed in T_4SNa and DbSNa solution, respectively, is associated with the length of the alkyl substituent on the benzene ring. The longer dodecyl group is believed to plasticize the polypyrrole interphases, resulting in smooth morphology and lower surface energy. The polypyrrole interphases formed in T_4SNa solution have microspheroidal morphology and high surface free energy. The surface energy of the polypyrrole-coated fibers were about 40% higher than the noncoated but surface oxidized commercial carbon fibers. It is expected that advanced compos-

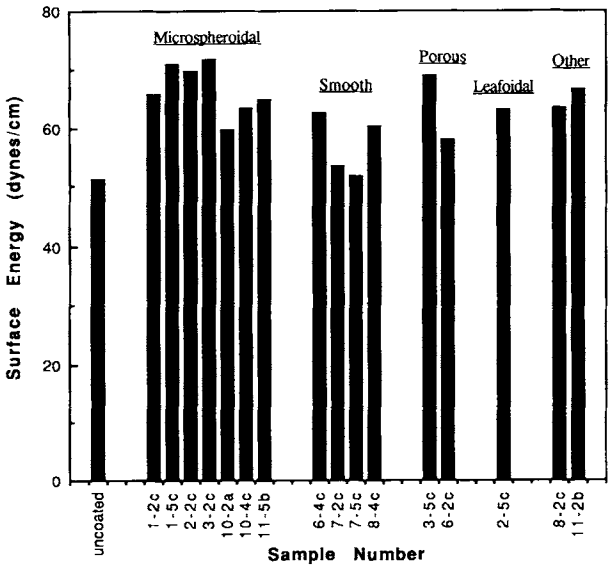

Figure 7 Dependence of the surface free energies of the polypyrrole–carbon fiber interphases on the surface morphology.

ites with superior interfacial properties will be produced by using the polypyrrole-coated carbon fibers.

REFERENCES

1. R. V. Subramanian, *Pure Appl. Chem.*, **52,** 1929–1937 (1990).
2. R. V. Subramanian and J. Jakubowski, *Polym. Eng. Sci.*, **18,** 590 (1978).
3. J. P. Bell, J. Chang, and H. W. Rhee, *Polym. Comp.*, **8,** 46 (1987).
4. J. P. Bell and H. W. Rhee, *SPE/ANTEC '88 Trans.*, 1590 (1990).
5. N. R. Sottos and R. McCullough, *Concepts in Fiber-Resin Composites,* Marcel Dekker, New York, 1971, p. 328.
6. B. D. Agarwal and L. J. Broutman, *Analysis and Performance of Fiber Composites,* Wiley, New York, 1990.
7. S. Wu, *Polymer Interface and Adhesion,* Marcel Dekker, New York, 1982, pp. 337–354.
8. L. H. Sharpe, *The Interfacial Interactions in Polymeric Composites,* G. Akovali, Ed., Kluwer, Netherlands, 1993, pp. 359–385.
9. J. Israelachvili, *Intermolecular and Surface Forces,* 2nd ed., Academic Press, San Diego, 1992.
10. S. Wu, *Polymer Interface and Adhesion,* Marcel Dekker, New York, 1982, pp. 12–15.
11. H. Simon, Ph.D. thesis, Universite' de Haute-Alsace, Mulhouse, France, 1984.
12. J. Schultz, L. Lavielle, and H. Simon, *Proc. Intl. Symp. Science and New Application of Carbon Fibers,* University of Toyohashi, Japan, Nov. 19–21, 1984, p. 125.
13. H. L. Cox, *Brit. J. Appl. Phys.*, **3,** 72 (1952).
14. J. N. Israelachvili, *Intermolecular and Surface Forces,* Academic Press, London, 1985.
15. L. T. Drzal, D. S. Grummon, R. Schalek, and A. Ozzello, *Modification of Fiber-Matrix Adhesion in Polyethylene Reinforced Composites by Energetic Ion Irradiation Conf. Proc.,* ASM, Detroit, 1990, pp. 155–162.
16. L. T. Drzal, M. J. Rich, M. Madhukar, and P. Herrera-Franco, *Characterization of Fiber-Matrix Adhesion in Composite Materials Conf. Proc.,* ASM, Detroit, 1990, pp. 155–162.
17. D. H. Kaelble and P. J. Dynes, *J. Adhesion,* **6,** 239–258 (1974).
18. B. Tissington, G. Pollard, and I. M. Ward, *J. Mat. Sci.*, **26,** 82–92 (1991).
19. H. D. Wagner, *J. Appl. Phys.*, **67**(3) (1990).
20. H. T. Chiu and J. S. Lin, *J. Mat. Sci.*, **27,** 319 (1992).
21. W. Yuan, MS Thesis, University of Cincinnati, 1994.
22. R. A. Jones, Ed., *Heterocyclic Compounds, Pyrroles,* Vol. 48, Part 1, Wiley, New York, 1990, p. 61.
23. C. J. Pouchert, *The Aldrich Library of IR Spectra,* 2nd Ed., Aldrich Chemical Co., Milwaukee, WI, 1975.
24. R. A. Meyers, Ed., *Encyclopedia of Physical Science and Technology,* Academic Press, Orlando, 1987, pp. 645–647.
25. N. B. Colthup, L. H. Daly, and S. E. Wiberley, *Introduction to Infrared and Raman Spectroscopy,* 3rd ed., Academic Press, San Diego, 1990, p. 464.
26. A. F. Diaz, R. Hernandex, R. Waltman, and J. Bargon, *J. Phys. Chem.*, **88,** 3333–3337 (1984).
27. G. A. Wood, M.S. thesis, University of Cincinnati, 1995.

Received March 18, 1996
Accepted June 21, 1996